Low-Voltage-Triggered Rapid Electrical Detachment of Pressure-Sensitive Adhesives via Ion Transport Channels

Zhijun Liu[a,c,d,e], Fei Cheng[b], Guoming Yuan[a,c,d,e], Yanhan Tao[a,c,d,e], Yihao Yang[a,c,d,e], Bo Yang[a,c,d,e], Kun Wu[a,e*], Jun Shi[a,e], Guangwen Che[a,e]

a Guangzhou Institute of Chemistry, Chinese Academy of Sciences, Guangzhou 510650, PR China. Email: wukun@gic.ac.cn; Fax: +86-20-85231925; Tel: +86-20-85231925.
b National Key Laboratory of Advanced Polymer Materials，Polymer Research Institute of Sichuan University，Chengdu
c CAS Engineering Laboratory for Special Fine Chemicals, Guangzhou 510650, China.
d CASH GCC Shaoguan Research Institute of Advanced Materials, Nanxiong 512400, PR China.
e University of Chinese Academy of Sciences, Beijing 100049, PR China.

Experimental Section

Materials characterization

The structure of the material was verified using a Fourier Transform Infrared (FTIR) Spectrometer (Thermo Fisher Nicolet IS 50/6700). The scanning range was 4000 cm^{-1} to 400 cm^{-1}, with a resolution of 4 cm^{-1} and a scanning frequency of 32 times.

The glass transition temperature (T_g) of the sample was measured using a Differential Scanning Calorimeter (DSC 2500, TA Instrument). The heating rate was 10 °C/min, and the testing temperature range was -80 ~ 100 °C.

Thermogravimetric analysis (TGA 5500 (TA Instrument)) was used to analyze the thermal decomposition performance of the samples. The samples were heated in a nitrogen atmosphere at a heating rate of 10 °C/min, with the temperature range from room temperature to 600 °C.

The electrochemical impedance spectroscopy (EIS) test of polyacrylate-based EDPSA was conducted using an electrochemical workstation (CHI660E). The frequency was set to 0.1 Hz - 2 MHz, and the voltage amplitude was set to 5 mV. The ion transfer resistance (Rb) of EDPSA was obtained, and then the ionic conductivity (σ) was calculated using Equation (1):

$$\sigma = \frac{I}{A \cdot Rb} \#\ (1)$$

Among them, I represents the thickness of polyacrylate-based EDPSA (20 μm), and A represents the bonding area of EDPSA.

Cyclic Voltammetry (CV) tests of polyacrylate-based EDPSA were performed using an electrochemical workstation (CHI660E). The scan rate was 2 mV/s, and the voltage range was 0-10 V. For each sample, 3 sets of data were collected, and the results were reported as the average value.

Linear Sweep Voltammetry (LSV) tests of EDPSA were conducted using an

electrochemical workstation (CHI660E). The voltage scan range was 0-10 V, and the scan rate was 0.1 V/s. For each sample, 3 sets of data were collected, and the results were reported as the average value.

The tack of PSA and EDPSA was tested using a universal tensile testing machine (YZHC-27200N) in accordance with the GB4852-2002 standard. For each sample, 3 sets of data were collected, and the results were reported as the average value.

The 180° peel strength of polyacrylate-based EDPSA was tested using a universal tensile testing machine (YZHC-27200N) in accordance with the GB/T 2792-2014 standard. For each sample, 3 sets of data were collected, and the results were calculated as the average value. The electrical separation efficiency (Ψ) is defined to describe the electrical separation behavior of polyacrylate-based EDPSA adhering to the substrate, and Ψ can be obtained using Equation (2):

$$\Psi_{[\alpha V,\beta s]} = 1 - \frac{F_{initial} - F_{residual}}{F_{initial}} x\ 100\%\#(2)$$

Among them, $F_{initial}$ represents the initial peeling force of EDPSA; $F_{residual}$ represents the residual peeling force of EDPSA after energization; α represents the value of the DC voltage applied during energization; and β represents the energization time.

The glass transition temperature (T_g) of the sample was measured using a Differential Scanning Calorimeter (DSC 2500, TA Instrument). The heating rate was 10 °C/min, and the testing temperature range was -80 ~ 100 °C.

The electrostatic surface potential (ESP) and binding energy (Ebinding) of the molecules were calculated using Density Functional Theory (DFT) with the Gaussian 16 software. The B3LYP functional and the 6-311G(d,p) basis set were employed for these calculations. The atom-pairwise dispersion correction with the DFT-D3(BJ) method (which introduces the Becke-Johnson damping function to the DFT-D3 correction) was incorporated during the optimization process to address the inherent limitation of DFT in accurately describing weak intermolecular interactions (such as van der Waals forces), thereby ensuring that the optimized geometries are closer to reality. The final results were visualized using Multiwfn and VMD software[1-3].

The basis set superposition error (BSSE) in the binding energy ($E_{binding}$) calculation was eliminated using the counterpoise method (to avoid the systematic error of an artificially more negative binding energy caused by the "overlap coverage" of basis sets of different components within the complex). The $E_{binding}$ was calculated using Equation (5).

$$E_{binding} = E_{AB} - E_A - E_B - BSSE\#(5)$$

where EA, EB, and EAB re the single-point energies of the isolated component A, the isolated component B, and the formed complex (A-B), respectively.

Scanning Electron Microscopy (SEM): A Philips XL30 microscope (Bruker Nano Berlin, Germany) was used to observe the sample morphology. X-ray Photoelectron Spectroscopy (XPS): Surface elemental analysis was performed on a Thermo Scientific K-Alpha spectrometer (USA).

X-ray Diffraction (XRD): Patterns were acquired using a Bruker D8 ADVANCE diffractometer.

Small-Angle X-ray Scattering (SAXS): A Xenocs Xeuss 3.0 instrument (France) was employed to analyze the phase structure.

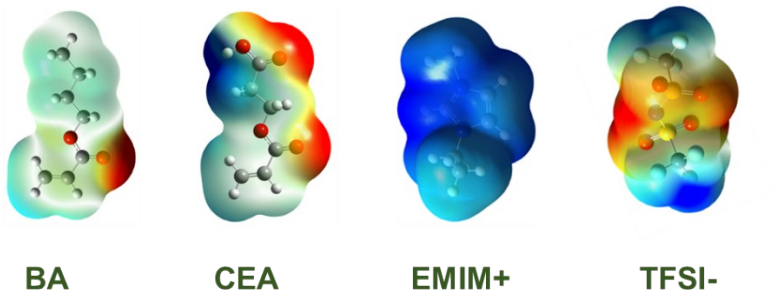

Figure S1. The ESP mappings of BA, CEA, [TFSI]-, [EMIM]+.

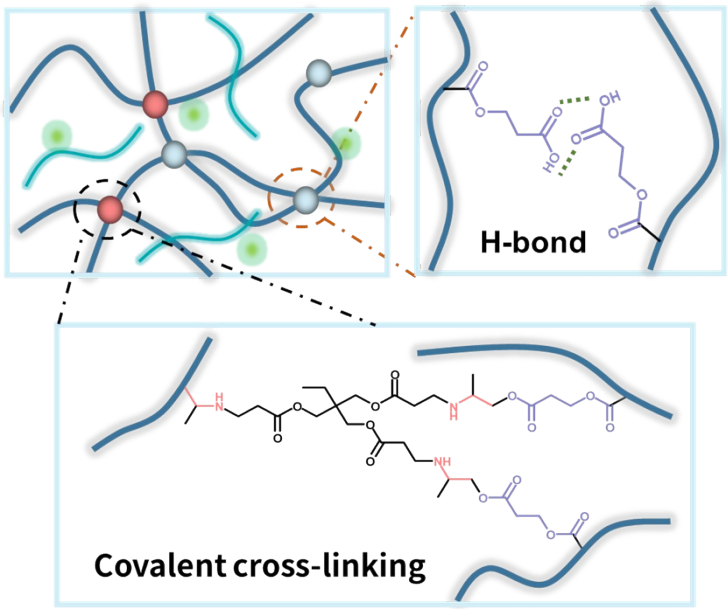

Figure S2. The cross-linking process of molecular chains.

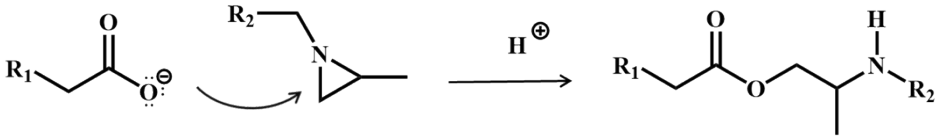

Figure S3. Mechanism of reaction between aziridine and carboxyl

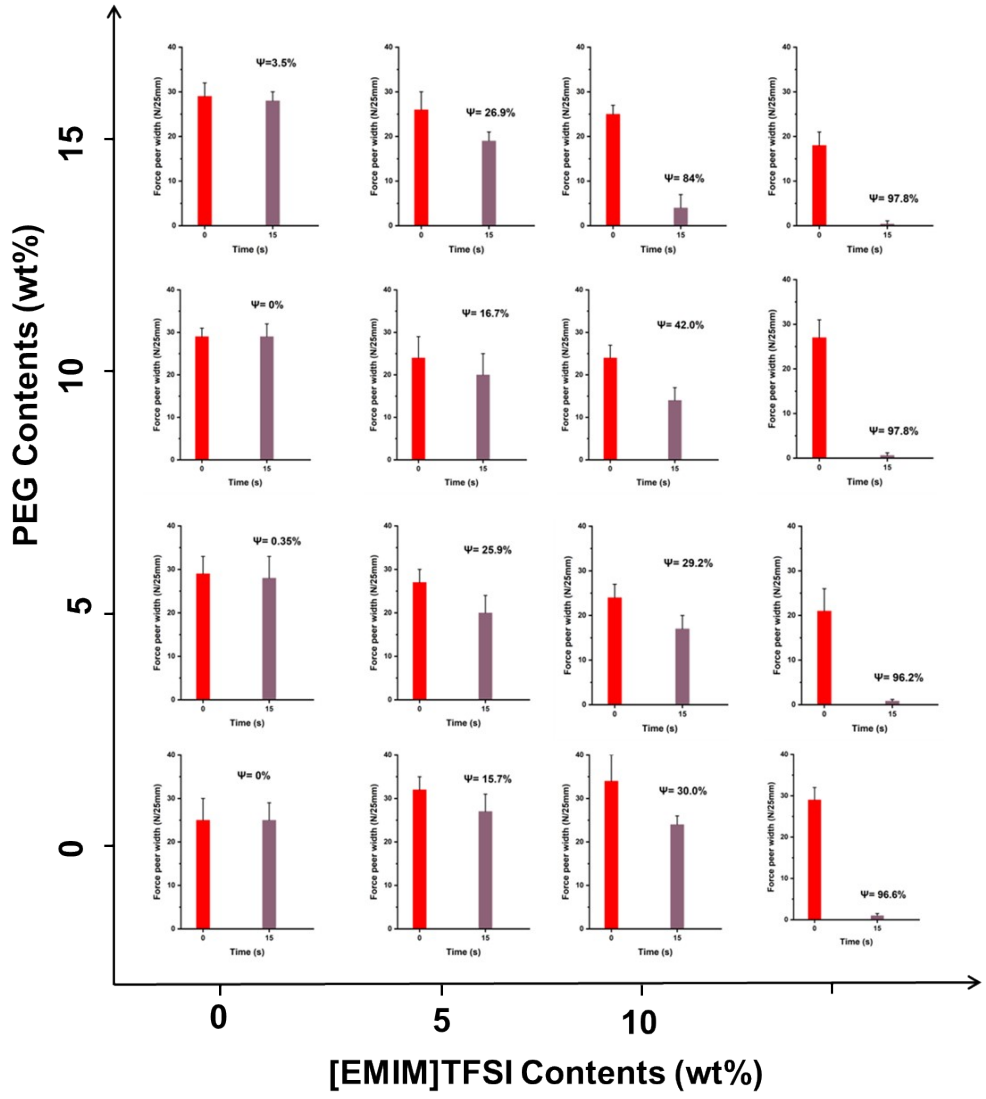

Figure S4. The electrically detaching behavior of $PSA_{Px\text{-}Iy}$ under 10 V DC voltage.

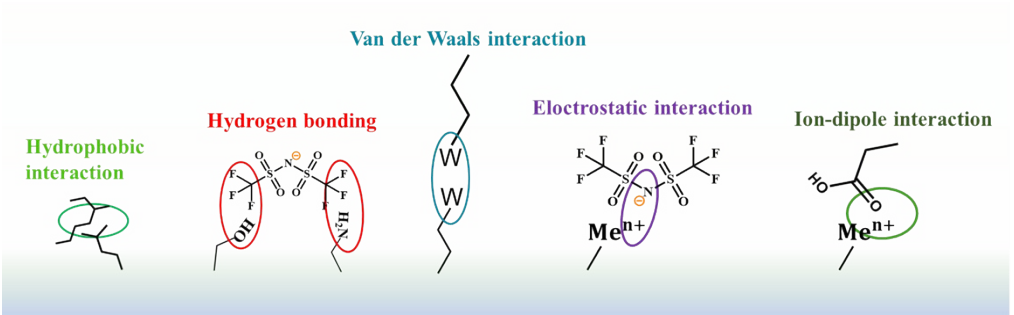

Figure S5. Schematic illustration of the tough adhesion, electrical detachment, and full recyclability of EDPSA tape adhesion.

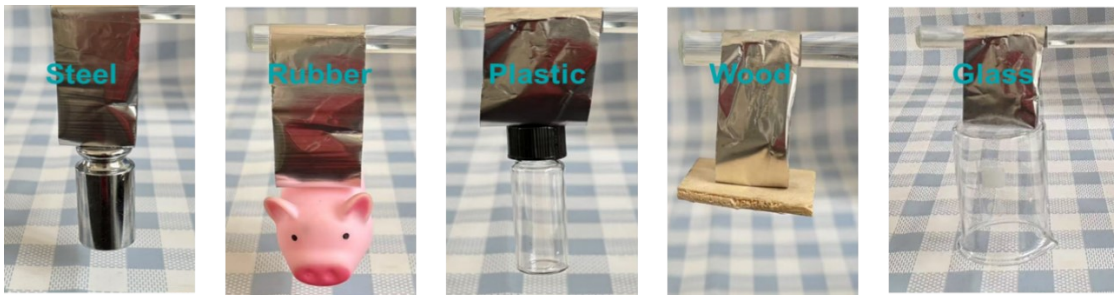

Figure S6. Adhesion digital images of PSAP10-I15 on different substrates, including weight, rubber, plastic, wood, glass.

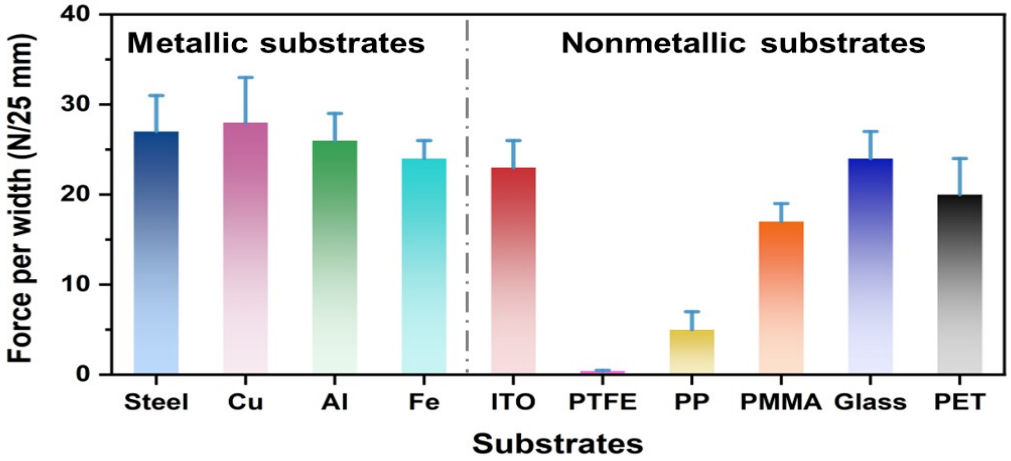

Figure S7. The peel strength of $PSA_{P10\text{-}I15}$ on different substrates.

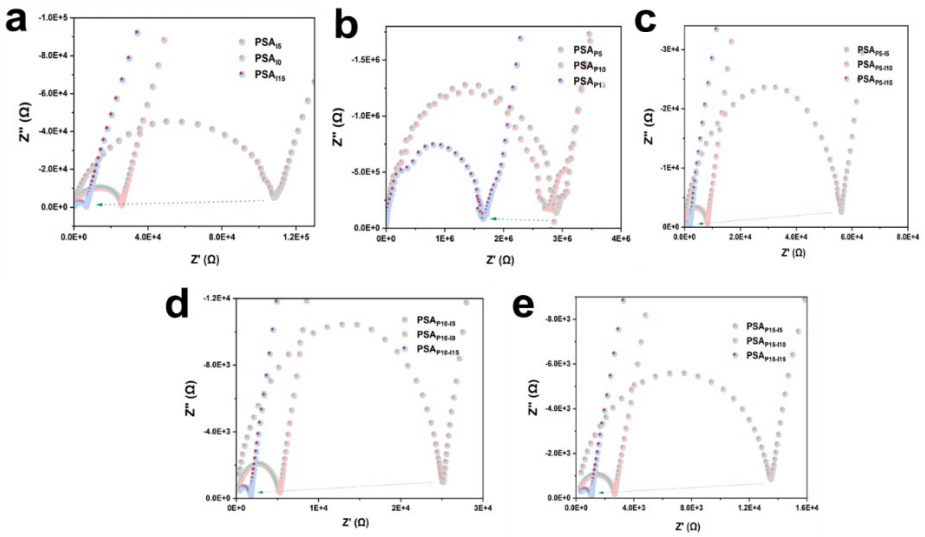

FigureS8. (a-e) The Nyquist curves of PSAPx-Iy.

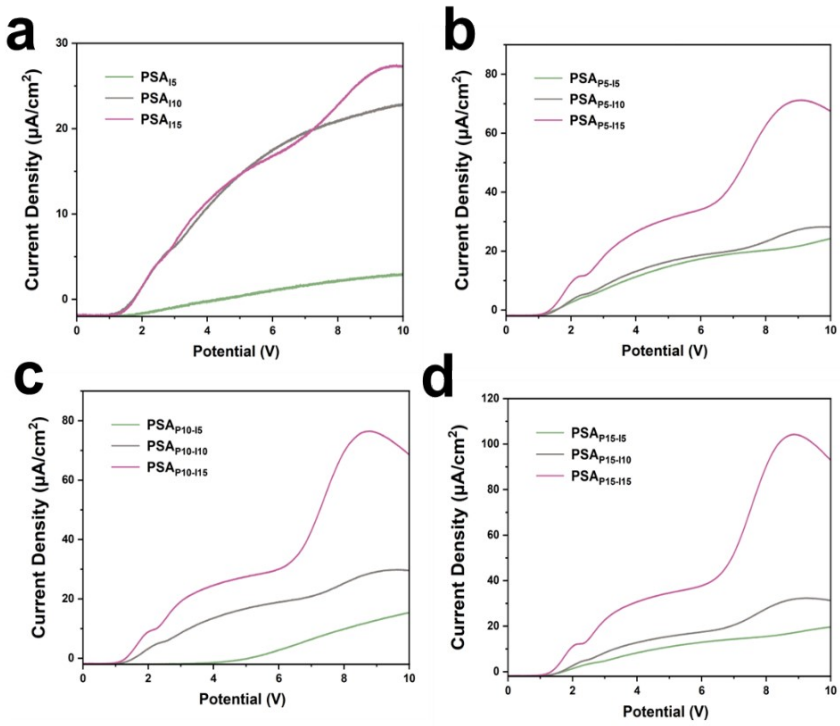

FigureS9. The LSV curves of PSAPx-Iy.

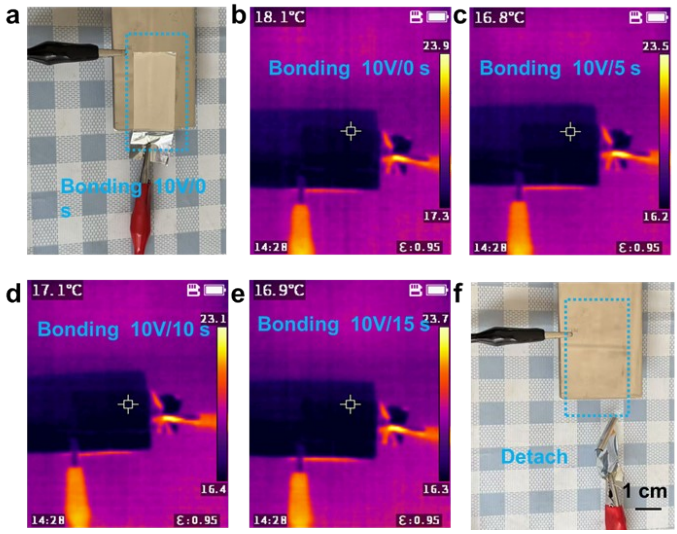

Figure S10. The infrared thermal images of EDPSA during the electrically detaching process at 10 V DC voltage, (a) 0 s, (b) 5 s, (c) 10 s, (d-e) 15 s

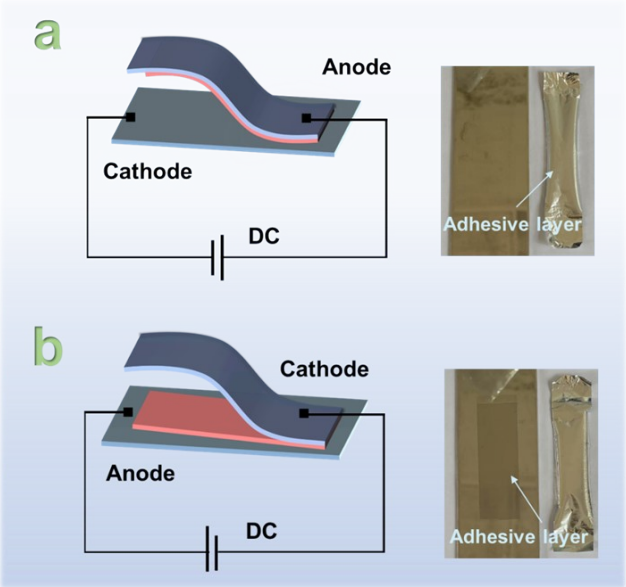

Figure S11. By switching the direction of the electric current, the adhesive interface can be selectively separated at either the cathode or the anode. (a) Separation at the cathode interface; (b) Separation at the anode interface.

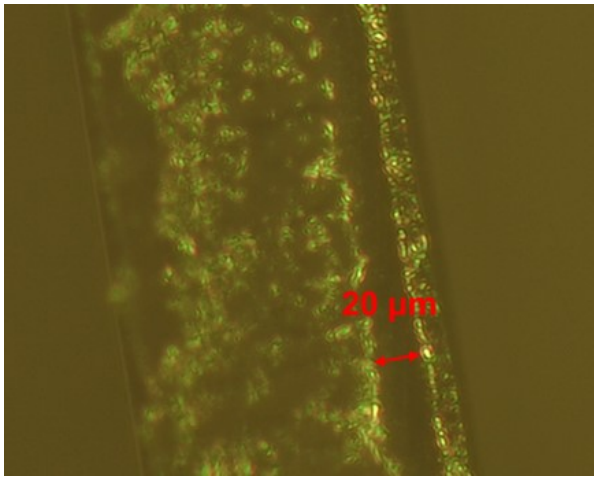

Figure S12. The OM images to show the $PSA_{P10\text{-}I15}$ thickness during the peel test.

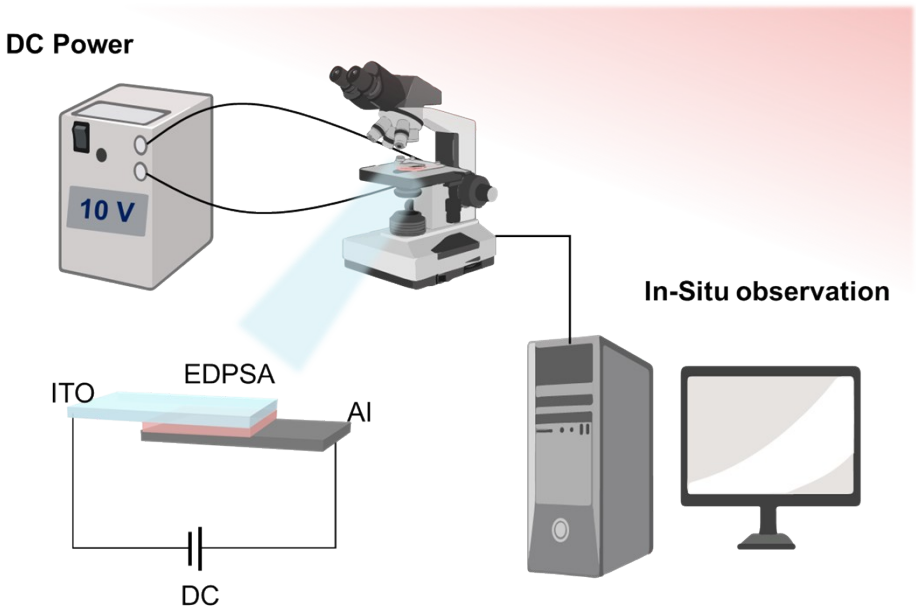

Figure S13 Schematic of the in-situ observation of the electrical detachment.

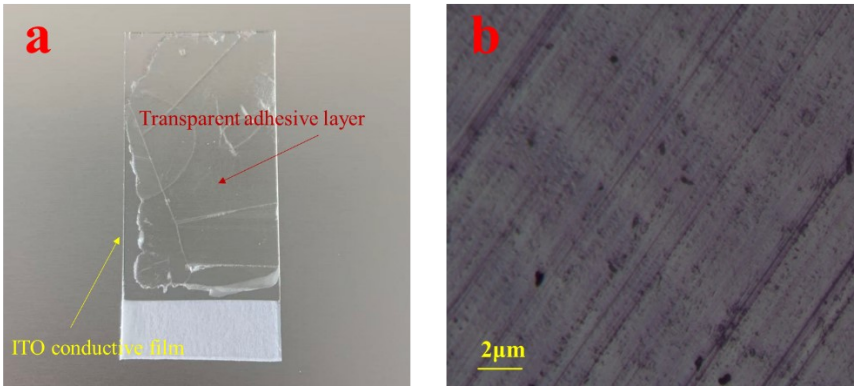

S14 a) A digital photograph of $PSA_{P10\text{-}I15}$. b) Optical microscope (OM) images of $PSA_{P10\text{-}I15}$.

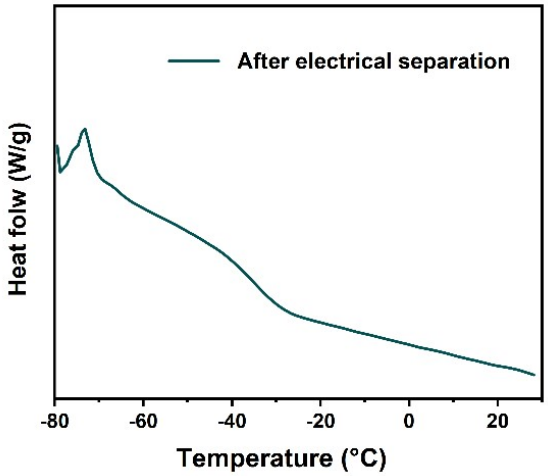

Figure S15 DSC curves of $PSA_{P10\text{-}I15}$ after different electrical detachment.

Table S1 Weight fraction of elements on the surface of adhesive layers after different electrical detachment.

Elements	Pristine content (wt%)	Anode content (wt%)	Cathode content (wt%)
C	56.9	62.66	64.22
N	12.84	15.62	16.63
O	25.15	16.67	15.61
F	3.61	3.46	1.21
AI	0.05	0.05	1.63
S	1.44	1.53	0.7

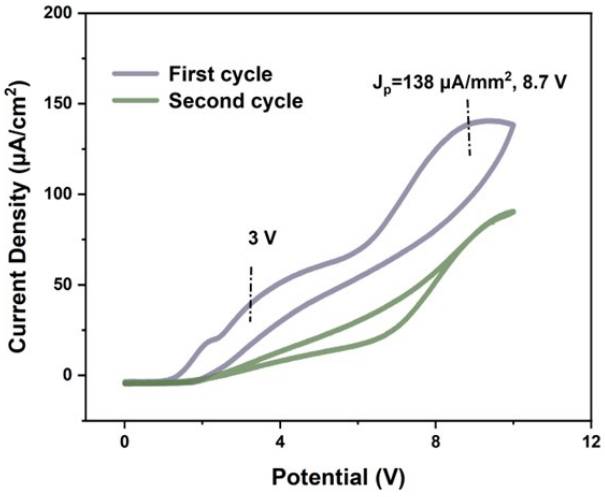

Figure S16. The CV curves of PSA_{I15}.

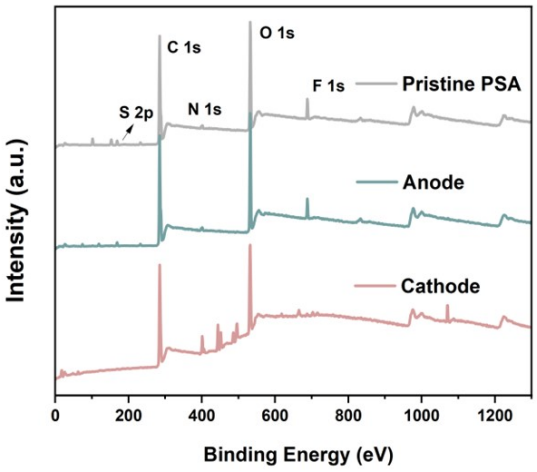

S17 X-ray photoelectron spectroscopy spectrum of $PSA_{P10\text{-}I15}$.

Table S2. Single-point energies, BSSE, $E_{binding}$ and configurations of BA, CEA, $EMIM^+$, $TFSI^-$ and the complexes.

Categories	Single-point Energy (Hartree)	BSSE (Hartree)	$E_{binding}$ (kCal/mol)	Configuration
BA	-424.3839713	/	/	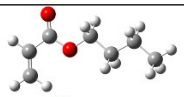
CEA	-534.3500016	/	/	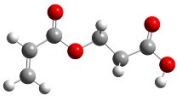
EMIM+	-344.5120736	/	/	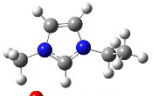
TFSI-	-1827.439478	/	/	
BA-C=O···EMIM$^+$	-768.9159076	0.000340575	-12.3	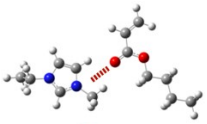
CEA -C=O···EMIM$^+$	-878.892969	0.0004853	-19.1	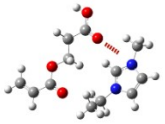
TFSI$^-$···EMIM$^+$	-2171.809301	0.072963137	-446.2	
CEA-C=O···TFSI$^-$(H-bond)	-2361.821743	0.001461191	-19.3	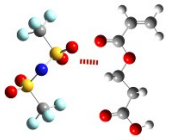
CEA-COOH···HOOC-CEA(Single)	-1068.713043	0.000620328	-7.8	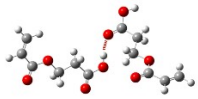
CEA-COOH···HOOC-CEA(Double)	-1068.74244	0.000741554	-26.2	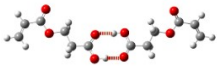

1. Lu, T.; Chen, F., Multiwfn: A multifunctional wavefunction analyzer. *Journal of Computational Chemistry* **2012,** *33* (5), 580-592.

2. Humphrey, W.; Dalke, A.; Schulten, K., VMD: visual molecular dynamics. *J Mol Graph* **1996,** *14* (1), 33-8, 27-8.

3. Yue, Q.; Lv, J.; Huang, S.; Guo, Y.; Wang, Y.; Liu, J.; Sun, S.; Wang, M.; Wang, S.; Wei, Y., Electrically Detachable and Fully Recyclable Pressure Sensitive Ionoadhesive Tapes. *Advanced Functional Materials* **2025,** *35* (22), 2423865.